

# The recent breakup of an asteroid in the main-belt region

David Nesvorný, William F. Bottke Jr, Luke Dones & Harold F. Levison

Southwest Research Institute, 1050 Walnut St, Suite 426, Boulder, Colorado 80302, USA

The present population of asteroids in the main belt is largely the result of many past collisions<sup>1,2</sup>. Ideally, the asteroid fragments resulting from each impact event could help us understand the large-scale collisions that shaped the planets during early epochs<sup>3–5</sup>. Most known asteroid fragment families, however, are very old and have therefore undergone significant collisional and dynamical evolution since their formation<sup>6</sup>. This evolution has masked the properties of the original collisions. Here we report the discovery of a family of asteroids that formed in a disruption event only  $5.8 \pm 0.2$  million years ago, and which has subsequently undergone little dynamical and collisional evolution<sup>6,7</sup>. We identified 39 fragments, two of which are large and comparable in size (diameters of  $\sim 19$  and  $\sim 14$  km), with the remainder exhibiting a continuum of sizes in the range 2–7 km. The low measured ejection velocities suggest that gravitational re-accumulation after a collision may be a common feature of asteroid evolution. Moreover, these data can be used to check numerical models of larger-scale collisions<sup>8</sup>.

Up to now, ejecta from a few tens of major collisions (that is, asteroid families) have been observed in the main belt<sup>9,10</sup>. To identify an asteroid family, researchers look for clusters of asteroid positions in the space of so-called proper orbital elements: the proper semimajor axis ( $a_p$ ), proper eccentricity ( $e_p$ ) and proper inclination ( $i_p$ ). The orbital elements describe the size, shape and tilt of orbits. Proper orbital elements, being more constant over time than instantaneous orbital elements<sup>11</sup>, provide a dynamical criterion of whether or not a group of bodies has a common ancestor. Unfortunately, the observed asteroid families are old enough (that is, hundreds of millions to billions of years old<sup>6,12</sup>) to have been substantially eroded and dispersed by: (1) secondary collisions<sup>5</sup>, (2) chaotic orbital evolution<sup>12,13</sup>, and (3) semimajor axis mobility due to radiation effects<sup>7</sup>. These effects make it difficult to determine the conditions that existed immediately after the family breakup event and the age of the family itself.

Fragments produced by recent collisions, on the other hand, would suffer little erosion in the interim following a breakup event, and thus would provide better examples for understanding impact physics than older families. To search for recently formed asteroid families, we applied a cluster-detection algorithm called the hierarchical clustering method<sup>9</sup> (HCM) to a proper-element database<sup>11,14</sup>. The output of the HCM algorithm is a number of clusters in the ( $a_p, e_p, i_p$ ) space. Each cluster consists of member bodies linked by a ‘chain’ in the ( $a_p, e_p, i_p$ ) space, with the length of each link,  $d$  (see Methods section), corresponding to a proper-element difference not exceeding  $d_{\text{cutoff}}$ . In order to detect signatures of compact, and presumably young, collisional clusters, we used  $d_{\text{cutoff}} = 10 \text{ m s}^{-1}$ . This value is an order of magnitude less than what is usually used for asteroid family searches.

The HCM algorithm found nine clusters with five or more member asteroids. Among them, four clusters form a prominent compact feature of 39 bodies within the region known as the Koronis family (Fig. 1). At  $d_{\text{cutoff}} = 15 \text{ m s}^{-1}$ , the four clusters join together, but also agglomerate a dozen additional asteroids, forming a similar but more loosely connected structure. In this work, we analyse the orbital and size-frequency distribution of the 39 asteroids detected at  $d_{\text{cutoff}} = 10 \text{ m s}^{-1}$ . This 39-body cluster is statistically significant at greater than the 99% level

(see Methods section).

The orbital distribution of the 39-body cluster is diagonally shaped in ( $a_p, e_p$ ), and appears to fit inside one of the similarly shaped ‘equivelocity’ ellipses shown in Fig. 1. To create these ellipses, we launched test bodies isotropically from the centre of the cluster (presumably the impact site) at a selected velocity impulse  $\delta V$ . Using Gauss’s equations (see, for example, ref. 14), we then computed the change in their proper elements ( $\delta a_p, \delta e_p, \delta i_p$ ). To determine the size, shape and orientation of the ellipses, we experimented with various values of  $V_{\text{max}}$ , the maximum velocity among our test bodies, the true anomaly  $f$  of the parent body (that is, the angle between the parent body’s location and the perihelion of its orbit) and the parent body’s perihelion argument  $\omega$  at the instant of the impact (that is, the angle between the perihelion and the ascending node).

We found that ellipsoids having  $V_{\text{max}} \approx 15 \text{ m s}^{-1}$ ,  $-30^\circ \leq f \leq 30^\circ$  and  $-45^\circ \leq \omega + f \leq 45^\circ$  provide good fits to our 39-body cluster (Fig. 1). These results indicate that the disruption event occurred while the parent body was near perihelion, and that the fragments were ejected in nearly isotropic directions.

No other known asteroid family shows a comparable fit to that shown in Fig. 1a. Instead, most observed families have box-like shapes in ( $a_p, e_p, i_p$ ) space. We believe these observed family configurations are by-products of long-term dynamical evolution<sup>7,13</sup> rather than the result of an unusual  $\delta V$  distribution. Similarly, our numerical experiments suggest that the structure of the 39-body cluster in ( $a_p, e_p, i_p$ ) space cannot be older than a few times  $10^7$  years, or it would have been erased by asteroid mobility

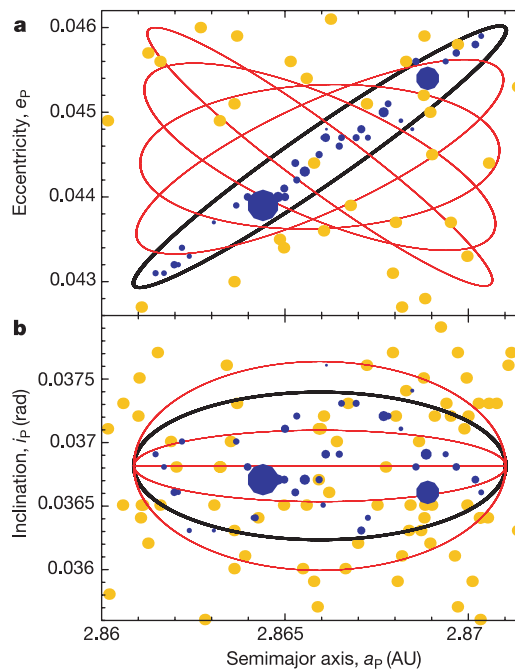


**Figure 1** The asteroid family in orbital phase space. The orbital structure of the identified cluster is compatible with a recent asteroid breakup at its location: **a**,  $a_p$  and  $e_p$ ; **b**,  $a_p$  and  $i_p$ . The size of each blue symbol is proportional to the diameter of a body. Gold dots indicate the background bodies in the Koronis family. The equivelocity ellipses were computed from Gauss’s equations. The red ellipses correspond to isotropic ejection fields with  $\delta V = 15 \text{ m s}^{-1}$  and different values of  $f$  and  $\omega$  (see text). In **a**,  $f = 30^\circ$  (black),  $60^\circ$ ,  $90^\circ$ ,  $120^\circ$  and  $150^\circ$  are shown. In **b**, the equivelocity ellipses were computed for  $\omega + f = 0^\circ, 45^\circ$  (black),  $70^\circ$  and  $90^\circ$ . The diagonal shape of the 39-body cluster in the ( $a_p, e_p$ ) plane suggests that the collision occurred near the perihelion of the parent’s body orbit. The overall structure in ( $a_p, e_p, i_p$ ) provides a reasonable match to the ellipses with parameters  $\delta V \leq 15 \text{ m s}^{-1}$ ,  $-30^\circ \leq f \leq 30^\circ$  and  $-45^\circ \leq \omega + f \leq 45^\circ$ .

mechanisms<sup>7,13</sup>. Thus, we conclude that the 39-body cluster must be young—so young, in fact, that it may be the first essentially unaltered disruption structure ever identified in the main belt.

To determine the age of the cluster, we numerically integrated the orbits of our 39 bodies into the past. Our goal was to show that in some previous epoch, the heliocentric orbits of all cluster members were nearly the same. As  $\delta V \ll V_{\text{orb}}$ , where  $V_{\text{orb}}$  is the orbital velocity of cluster members, we expect that this conjunction of orbital elements should have occurred shortly after the parent body disrupted.

There are two angles that determine the orientation of an orbit in space: the longitude of the ascending node ( $\Omega$ ), and the argument of perihelion ( $\omega$ ). Owing to planetary perturbations, these angles evolve with different but nearly constant speeds for individual asteroid orbits (for example, precession periods of  $\sim 19,000$  yr and  $9,500$  yr, respectively, for cluster members). Today, the orbits of the cluster members are oriented differently in space because their slightly dissimilar periods of  $\Omega$  and  $\omega$  produce slow differential rotation of their orbits with respect to each other. Eventually, this effect allows  $\Omega$  and  $\omega$  to obtain nearly uniform distributions in  $[0^\circ, 360^\circ]$ . For a short time after the parent body breakup, however, the orientations of the fragments' orbits must have been nearly the same.

To deal solely with well-determined orbits, we used the orbital elements of the 13 cluster members that have a number designation<sup>16</sup>. The orbits were propagated backward in time using a symplectic integration scheme (the Wisdom–Holman map in the software package Swift<sup>17,18</sup>) with a 0.01-year step size. The inte-

gration accounted for the gravitational effect of the four giant planets, but neglected the effect of the inner planets, radiation forces and relativistic corrections. Given the small eccentricities and inclinations of the cluster, its location in a regular part of the main belt and the short integration interval, the latter effects can be ignored. We nevertheless verified that the inclusion of the inner planets in the integration did not change our results.

We find that about 5.8 Myr ago, all integrated orbits had nearly the same orientation in space (Fig. 2). This convergence did not happen by chance; we estimate that the probability that 13 unrelated orbits would randomly meet at one time over the age of the Solar System is  $< 10^{-6}$ . We also tested this idea by integrating their orbits forwards and backwards by 50 Myr. No other alignment was found. Thus, we conclude that the cluster members had a common collisional origin about 5.8 Myr ago.

To roughly estimate the error on this age ( $\Delta t$ ), we did the following. First, we computed the angular distance between the cluster members' ascending nodes at various times ( $t = -5.8 \pm \Delta t$ ). Next, we averaged these values for each  $t$ . The minimum average value, found at  $t = -5.8$  Myr, was about  $10^\circ$ . For  $\Delta t = 0.2$  Myr, the average angular distance had doubled to  $20^\circ$ . Thus, we estimate that the breakup event occurred  $5.8 \pm 0.2$  Myr ago.

The size–frequency distribution of the 39-body cluster shows two large bodies, (832) Karin and (4507) 1990 FV, with absolute magnitudes  $H = 11.2$  (diameter  $D \approx 19$  km for a 16% albedo) and  $11.8$  ( $D \approx 14.4$  km), respectively. As (832) Karin is the largest body in the observed population, we adopt the name 'Karin cluster'. The Karin cluster's size–frequency distribution shows 6, 15, 11, 3 and 2 bodies in 0.5-mag bins between  $H = 13.5$  mag and  $16.0$  mag ( $D \approx 6.6$ – $2.1$  km). The size–frequency distribution of this continuum is strongly affected by observational incompleteness.

To compute the size of the parent body of the Karin cluster, we need to account for its undetected members. Using a reasonable estimate of the observational incompleteness of the main belt for asteroids with  $H < 16.0$  mag (ref. 19), we infer that the diameter of the parent body was  $D_{\text{PB}} \approx 24.5 \pm 1$  km.  $D_{\text{PB}}$  corresponds to a spherical body with volume equal to the estimated total volume of the bodies with  $H < 16.0$  mag. It is likely that the actual size of the parent body was larger than  $D_{\text{PB}}$  because the contribution of the population at  $H > 16.0$  mag was not used. According to the above estimate, (832) Karin contains  $47 \pm 6\%$  of the mass of the parent body. The estimated disruption rate of asteroids in the main belt with  $D \approx 25$  km (1 per  $\sim 5$  Myr) is consistent with our derived age for the Karin cluster (D. Durda, personal communication).

According to numerical models<sup>8</sup>, an impact at  $5 \text{ km s}^{-1}$  of a  $\approx 3$ -km-diameter projectile on the 24.5-km-diameter parent body of the Karin cluster produces a fragment comparable to the size of (832) Karin. The next largest Karin cluster member, however, is only  $\sim 25\%$  smaller than (832) Karin itself. Because impacts onto solid homogeneous parent bodies are thought to yield large fragments with significant diameter differences<sup>2</sup>, these measurements suggest that either the parent body was fractured before the breakup event or the parent body had a heterogeneous interior structure.

Another possibility is that low ejection velocities allowed gravitational reaccumulation to modify the sizes of the largest fragments. Assuming  $f = \pm 30^\circ$  and  $\omega + f = \pm 45^\circ$ , we invert Gauss's equations and find that typical  $\delta V$  values are  $\lesssim 15 \text{ m s}^{-1}$ . We also find a correlation between the calculated  $\delta V$  values and the size of a body, with  $\delta V \propto D^{-1}$ . These ejection velocities are comparable to the escape velocity of a spherical, 25-km-diameter body with a bulk density of  $2.5 \text{ g cm}^{-3}$  (that is,  $V_{\text{esc}} \approx 15 \text{ m s}^{-1}$ ). We expect that the largest cluster members will agglomerate fragments having ejection velocities  $V_{\text{ejc}} < V_{\text{esc}}$ , assuming reasonable distributions of  $V_{\text{ejc}}$  (ref. 20).

The relative youth and known age of the members of the Karin cluster may help us answer several important questions in asteroid

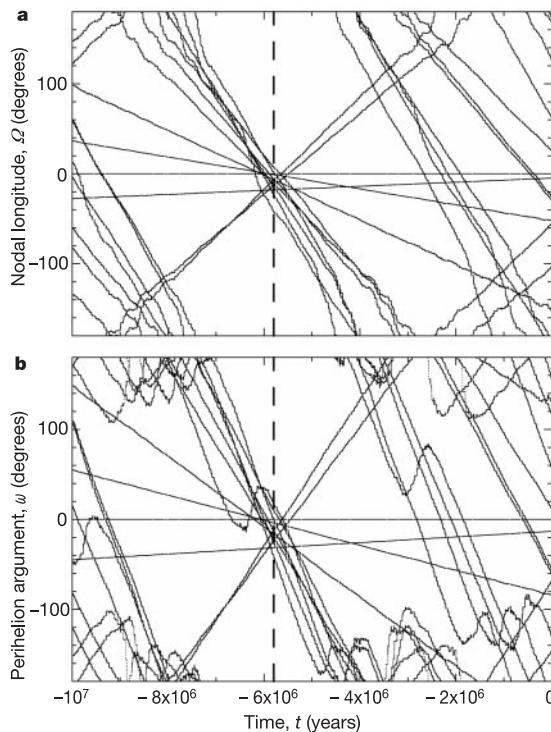


**Figure 2** The convergence of angles at about 5.8 Myr ago strongly suggests that the identified cluster was created by a recent catastrophic collision. The plot shows past orbital histories of the 13 numbered members of the 39-body cluster: **a**, nodal longitude  $\Omega$ , and **b**, perihelion argument  $\omega$ . Values relative to (832) Karin are shown. For clarity, the evolutions were smoothed by a 0.5-Myr running time window.  $\Omega$  and  $\omega$  have small oscillations about the average values. At  $t = -5.8$  Myr (broken vertical line), the nodal longitudes and perihelion arguments of all 13 asteroids were nearly the same. Thus, at  $t = -5.8$  Myr, all orbits were nearly identical.

geology and impact physics. Recent work has suggested that S-type asteroids with 'fresh' surfaces may have spectra that resemble (or trend towards) ordinary chondrite spectra (see, for example, ref. 21). Because Karin cluster asteroids are S-type<sup>22</sup> and have probably experienced minimal space weathering<sup>23</sup>, we believe they could be used to examine this possibility. It would also be useful to compare the spectra of various Karin cluster asteroids, all of which should share the same age (that is, 5.8 Myr). Similarities and differences might help us to determine the rate of space weathering among S-type main-belt asteroids, and whether spectral alterations by space weathering are a function of time alone or are also dependent on asteroid size. Moreover, if the surfaces of the Karin-cluster members were given fresh surfaces by impact 5.8 Myr ago, the craters formed since that time by hypervelocity impacts may be used to infer the current crater production rate in the main belt, and the unknown shape of the main-belt's size distribution at small asteroid sizes.

It is possible that the Karin cluster may be the source of some asteroidal material evolving towards Earth. For example, we believe that impacts on Karin cluster asteroids could be the source of the zodiacal dust  $\beta$ -band discovered by the IRAS satellite<sup>24</sup>. We base this idea on two pieces of evidence: (1) the Karin cluster and the model-derived source of the  $\beta$ -band both have mean inclinations near  $2.1^\circ$ , and (2) the narrow inclination span of the  $\beta$ -band source ( $\Delta i \approx 0.09^\circ$ ) is analogous to that of our compact 39-body cluster ( $\Delta i \approx 0.08^\circ$ )<sup>25</sup>. (The inclination span of the Koronis family, which has generally been taken as the source of the  $\beta$ -band, is  $\Delta i \approx 0.45^\circ$ ). As a second example, we believe the Karin breakup event could have produced some meteorites. These putative objects would need to have compositions consistent with S-type asteroids and cosmic-ray exposure<sup>26</sup> ages  $\approx 5.8$  Myr.  $\square$

## Methods

### Hierarchical clustering method

The hierarchical clustering method (HCM) starts with an individual asteroid position in the proper elements space, and identifies bodies in its neighbourhood with mutual distances less than a threshold limit ( $d_{\text{cutoff}}$ ). We define the distance in the  $(a_p, e_p, i_p)$  space by:

$$d = n a_p \sqrt{C_a (\delta a_p / a_p)^2 + C_e (\delta e_p)^2 + C_i (\delta \sin i_p)^2} \quad (1)$$

where  $n a_p$  is the heliocentric velocity of an asteroid on a circular orbit having the semimajor axis  $a_p$ .  $\delta a_p = |a_p^{(1)} - a_p^{(2)}|$ ,  $\delta e_p = |e_p^{(1)} - e_p^{(2)}|$ , and  $\delta \sin i_p = |\sin i_p^{(1)} - \sin i_p^{(2)}|$ . The indices (1) and (2) denote the two bodies under consideration.  $C_a$ ,  $C_e$  and  $C_i$  are constants: we use  $C_a = 5/4$ ,  $C_e = 2$  and  $C_i = 2$  (ref. 10). Other choices of these constants found in the literature yield similar results.

### Statistical significance of the 39-body cluster

To demonstrate the >99% statistical significance of the 39-body cluster, we generated 100 synthetic orbital distributions corresponding to the Koronis family determined at  $d_{\text{cutoff}} = 60 \text{ m s}^{-1}$  (that is, 1,500 asteroid positions at  $2.83 < a_p < 2.95 \text{ AU}$ ,  $0.04 < e_p < 0.06$  and  $0.033 < i_p < 0.04$ ), and applied our HCM algorithm to these data. Applying  $d_{\text{cutoff}} = 10 \text{ m s}^{-1}$ , we were unable to find a cluster containing more than five members. We also used the HCM algorithm on 100 computer-generated asteroid belts (that is, 66,000 random orbital positions at  $2.1 < a_p < 3.25 \text{ AU}$ ,  $e_p < 0.3$  and  $i_p < 0.3$ ). Once again,  $d_{\text{cutoff}} = 10 \text{ m s}^{-1}$  yielded no meaningful structures.

Received 27 February; accepted 11 April 2002; doi:10.1038/nature00789.

1. Durda, D. D., Greenberg, R. & Jedicke, R. Collisional models and scaling laws: a new interpretation of the shape of the main-belt asteroid size distribution. *Icarus* **135**, 431–440 (1998).
2. Michel, P., Benz, W., Tanga, P. & Richardson, D. C. Collisions and gravitational reaccumulation: Forming asteroid families and satellites. *Science* **294**, 1696–1700 (2001).
3. Zappalà, V., Cellino, A., Dell'Oro, A. & Paolicchi, P. in *Asteroids III* (eds Bottke, W. F., Cellino, A., Paolicchi, P. & Binzel, R.) (Univ. Arizona Press, in the press).
4. Chambers, J. E. & Wetherill, G. W. Making the terrestrial planets: N-body integrations of planetary embryos in three dimensions. *Icarus* **136**, 304–327 (1998).
5. Canup, R. M. & Asphaug, E. Origin of the Moon in a giant impact near the end of the Earth's formation. *Nature* **412**, 708–712 (2001).
6. Marzari, F., Davis, D. & Vanzani, V. Collisional evolution of asteroid families. *Icarus* **113**, 168–187 (1995).
7. Bottke, W. F., Vokrouhlický, D., Brož, M., Nesvorný, D. & Morbidelli, A. Dynamical spreading of asteroid families by the Yarkovsky effect. *Science* **294**, 1693–1696 (2001).
8. Benz, W. & Asphaug, E. Catastrophic disruptions revisited. *Icarus* **142**, 5–20 (1999).
9. Hirayama, K. Groups of asteroids probably by common origin. *Astron. J.* **31**, 185–188 (1918).
10. Zappalà, V., Cellino, A., Farinella, P. & Milani, A. Asteroid families. II. Extension to unnumbered multioppositional asteroids. *Astron. J.* **107**, 772–801 (1994).
11. Milani, A. & Knežević, Z. Asteroid proper elements and the dynamical structure of the asteroid main

belt. *Icarus* **107**, 219–254 (1994).

12. Milani, A. & Farinella, P. The age of the Veritas asteroid family deduced by chaotic chronology. *Nature* **370**, 40–41 (1994).
13. Nesvorný, D., Morbidelli, A., Vokrouhlický, D., Bottke, W. F. & Brož, M. The Flora family: a case of the dynamically dispersed collisional swarm? *Icarus* **157**, 155–172 (2002).
14. *Asteroids Dynamic Site* (<http://hamilton.dm.unipi.it/cgi-bin/astdys/astibo>) (7 May 2002).
15. Morbidelli, A., Zappalà, A., Moons, M., Cellino, A. & Gonczi, R. Asteroid families close to mean motion resonances: Dynamical effect and physical implications. *Icarus* **118**, 132–154 (1995).
16. *IAU: Minor Planet Centre* (<http://cfa-www.harvard.edu/cfa/ps/mpc.html>) (7 May 2002).
17. Levison, H. F. & Duncan, M. The long term dynamical behaviour of short-period comets. *Icarus* **108**, 18–36 (1994).
18. Wisdom, J. & Holman, M. Symplectic maps for the n-body problem. *Astron. J.* **102**, 1528–1538 (1991).
19. Jedicke, R. & Metcalfe, T. S. The orbital and absolute magnitude distributions of main belt asteroids. *Icarus* **131**, 245–260 (1998).
20. Fujiwara, A. et al. in *Asteroids II* (eds Binzel, R. P., Gehrels, T. & Matthews, M. S.) 240–265 (Univ. Arizona Press, Tucson, 1989).
21. Binzel, R. P., Bus, S. J., Burbine, T. H. & Sunshine, J. M. Spectral properties of near-earth asteroids: Evidence for sources of ordinary chondrite meteorites. *Science* **273**, 946–948 (1996).
22. (<http://pdssbn.astro.umd.edu/SBNast/holdings/EAR-A-5-DDR-UBV-MEAN-VALUES-V1.0.html>) (6 Feb. 2001).
23. Clark, B. E., Hapke, B., Pieters, C. & Britt, D. in *Asteroids III* (eds Bottke, W., Cellino, A., Paolicchi, P. & Binzel, R. P.) (Univ. Arizona Press, in the press).
24. Dermott, S. F., Nicholson, P. D., Burns, J. A. & Houck, J. R. Origin of the solar system dust bands discovered by IRAS. *Nature* **312**, 505–509 (1984).
25. Grogan, K., Dermott, S. F. & Durda, D. D. The size-frequency distribution of the zodiacal cloud: Evidence from the solar system dust bands. *Icarus* **152**, 251–267 (2001).
26. Marti, K. & Graf, T. Cosmic-ray exposure history of ordinary chondrites. *Annu. Rev. Earth Planet. Sci.* **20**, 221–243 (1992).

## Acknowledgements

We thank R. Binzel, C. Chapman, D. Durda, O. Eugster, B. Gladman, D. Hamilton, R. Jedicke, A. Morbidelli, F. Namouni and M. Sykes for their suggestions.

## Competing interests statement

The authors declare that they have no competing financial interests.

Correspondence and requests for materials should be addressed to D.N. (e-mail: davidn@boulder.swri.edu).

# Coulomb blockade and the Kondo effect in single-atom transistors

Jiwoong Park<sup>\*†‡</sup>, Abhay N. Pasupathy<sup>\*‡</sup>, Jonas I. Goldsmith<sup>§</sup>, Connie Chang<sup>\*</sup>, Yuval Yaish<sup>\*</sup>, Jason R. Petta<sup>\*</sup>, Marie Rinkoski<sup>\*</sup>, James P. Sethna<sup>\*</sup>, Héctor D. Abruña<sup>§</sup>, Paul L. McEuen<sup>\*‡</sup> & Daniel C. Ralph<sup>\*‡</sup>

<sup>\*</sup> Laboratory of Atomic and Solid State Physics; and <sup>§</sup> Department of Chemistry and Chemical Biology, Cornell University, Ithaca, New York 14853, USA

<sup>†</sup> Department of Physics, University of California, Berkeley, California 94720, USA

<sup>‡</sup> These authors contributed equally to this work

Using molecules as electronic components is a powerful new direction in the science and technology of nanometre-scale systems<sup>1</sup>. Experiments to date have examined a multitude of molecules conducting in parallel<sup>2,3</sup>, or, in some cases, transport through single molecules. The latter includes molecules probed in a two-terminal geometry using mechanically controlled break junctions<sup>4,5</sup> or scanning probes<sup>6,7</sup> as well as three-terminal single-molecule transistors made from carbon nanotubes<sup>8</sup>, C<sub>60</sub> molecules<sup>9</sup>, and conjugated molecules diluted in a less-conducting molecular layer<sup>10</sup>. The ultimate limit would be a device where electrons hop on to, and off from, a single atom between two contacts. Here we describe transistors incorporating a transition-metal complex designed so that electron transport occurs through well-defined charge states of a single atom. We examine two related molecules containing a Co ion bonded to polypyridyl ligands, attached to insulating tethers of different lengths. Chan-